# The Roles of Conserved Carboxylate Residues in IMP Dehydrogenase and Identification of a Transition State Analog†

Kathleen M. Kerr and Lizbeth Hedstrom*

*Department of Biochemistry, Brandeis University, Waltham, Massachusetts 02254*

*Received June 12, 1997; Revised Manuscript Received August 28, 1997*⊗

ABSTRACT: IMP dehydrogenase (IMPDH) catalyzes the oxidation of IMP to XMP with the concomitant reduction of $NAD^+$; the enzyme is activated by $K^+$. This reaction is the rate-limiting step in *de novo* guanine nucleotide biosynthesis. In order to identify functionally important residues in IMPDH, including those involved in substrate and $K^+$ binding, we have mutated 11 conserved Asp and Glu residues to Ala in *Escherichia coli* IMPDH. The values of $k_{cat}$, $K_m$, and $K_i$ for GMP, XMP, mizoribine 5′-monophosphate (MMP), and $\beta$-methylene-tiazofurin adenine dinucleotide (TAD) were determined. Five of these mutations caused a significant change (≥10-fold) in one of these parameters. The Asp248 → Ala mutation caused 100-fold decrease in the value of $k_{cat}$ and a 25-fold increase in the value of $K_{ii}$ for TAD; these observations suggest that Asp248 is in the $NAD^+$ binding site. The Asp338 → Ala mutation caused a 600-fold decrease in the value of $k_{cat}$, but only a 5−10-fold increase in the values of $K_m$ for IMP and $K_{is}$ for IMP analogs, suggesting that Asp338 may be involved in acid-base catalysis as well as IMP binding. The remaining three residues, Asp13, Asp50, and Glu469, appear to be involved in $K^+$ activation; these residues may be ligands at one or more $K^+$ binding sites. Interestingly, changes in the values of $K_i$ for MMP correlate with changes in $k_{cat}/K_mK_m$ of IMPDH, while no such correlation is observed for GMP, XMP, and TAD. This observation indicates that MMP is a transition state analog for the IMPDH reaction.

IMP dehydrogenase (IMPDH)[1] catalyzes the oxidation of IMP to XMP with the conversion of $NAD^+$ to NADH. This reaction controls the overall rate of *de novo* guanine nucleotide biosynthesis. Guanine nucleotides play a central role in cell growth processes, such as DNA and RNA biosynthesis, signal transduction, and tubulin assembly. Thus, IMPDH activity regulates cellular guanine levels and consequently affects cell proliferation (Weber, 1983). IMPDH inhibitors target rapidly proliferating cells and are potential therapeutics for cancer. Furthermore, IMPDH inhibitors ribavarin, mizoribine, and mycophenolate mofetil are currently used in antiviral and immunosuppressive therapies (Streeter et al., 1973; Robins, 1982; Allison, 1993). In addition, mammalian and microbial IMPDHs differ significantly in inhibitor sensitivity and catalytic efficiency, which suggests that IMPDH may be a target for anti-infective agents (Hupe et al., 1986; Verham et al., 1987; Wang et al., 1996). Overall, the potential therapeutic benefits from the investigation of the mechanism of IMPDH are clear. Our goal is to define functionally important residues in IMPDH.

A mechanism for the IMPDH reaction is shown in Figure 1. The reaction is initiated by the attack of Cys305 (*Escherichia coli* IMPDH numbering) on the 2 position of IMP forming a covalent E-IMP intermediate. In the subsequent step, hydride is transferred to $NAD^+$ producing NADH and an E-XMP* intermediate (Huete-Perez et al., 1995; Link & Straub, 1996; Sintchak et al., 1996). This intermediate is hydrolyzed to release XMP and regenerate the free enzyme. Two general acid-base catalysts are expected to be involved in the IMPDH mechanism: a general acid stabilizes the tetrahedral intermediates formed by the attack of Cys305 on IMP and by the attack of water on E-XMP* and a general base catalyst activates water. These residues have not been identified.

IMPDH is activated by monovalent cations. The extent of activation and cation specificity vary among IMPDHs from different sources (Anderson & Sartorelli, 1968; Powell et al., 1969; Heyde et al., 1976; Atkins et al., 1985; Xiang et al., 1996; Verham et al., 1987). $K^+$ is the most effective activator. *E. coli* IMPDH activity increases 100-fold in the presence of $K^+$, while only a 10-fold increase is observed in the activity of *Tritrichomonas foetus* (Verham et al., 1987; J. Digits and L. Hedstrom, unpublished observations). In general, larger cations, such as $Rb^+$, $NH_4^+$, and $Cs^+$, also activate IMPDH while smaller cations, such as $Li^+$ and $Na^+$, inhibit. The mechanism of monovalent cation activation of IMPDH is not understood: the stoichiometry of $K^+$ binding to IMPDH has not been determined nor have the ligands of the $K^+$ binding site(s) been identified.

Since active site residues are generally conserved throughout evolution, sequence alignments can provide clues to functionally important residues. Amino acid sequences are presently available for IMPDHs from 25 sources, including archae, eubacteria, and eukaryote organisms. Carboxylate

† Funded by NIH Molecular Structure and Function Training Grant GM07956 (K.M.K.) and a grant from the Lucille P. Markey Charitable Trust to Brandeis University. L.H. is a Searle Scholar and a Beckman Young Investigator. This manuscript is No. 1817 from the Department of Biochemistry, Brandeis University.

* To whom correspondence should be addressed.

⊗ Abstract published in *Advance ACS Abstracts,* October 15, 1997.

[1] Abbreviations: IMPDH, inosine 5′-monophosphate dehydrogenase; IMP, inosine 5′-monophosphate; $NAD^+$, nicotinamide adenine dinucleotide; NADH, reduced nicotinamide adenine dinucleotide; XMP, xanthosine 5′-monophosphate; GMP, guanosine 5′-monophosphate; MPA, mycophenolic acid; TAD, $\beta$-methylene tiazofurin adenine dinucleotide; MMP, mizoribine 5′-monophosphate; EDC, 1-ethyl-3-[3-(dimethylamino)propyl]carbodiimide; EICARMP, 5-ethynyl-1-$\beta$-D-ribofuranosylimidazole-4-carboxamide 5′-monophosphate; DTT, dithiothreitol; PAGE, polyacrylamide gel electrophoresis.

S0006-2960(97)01416-5 CCC: $14.00 

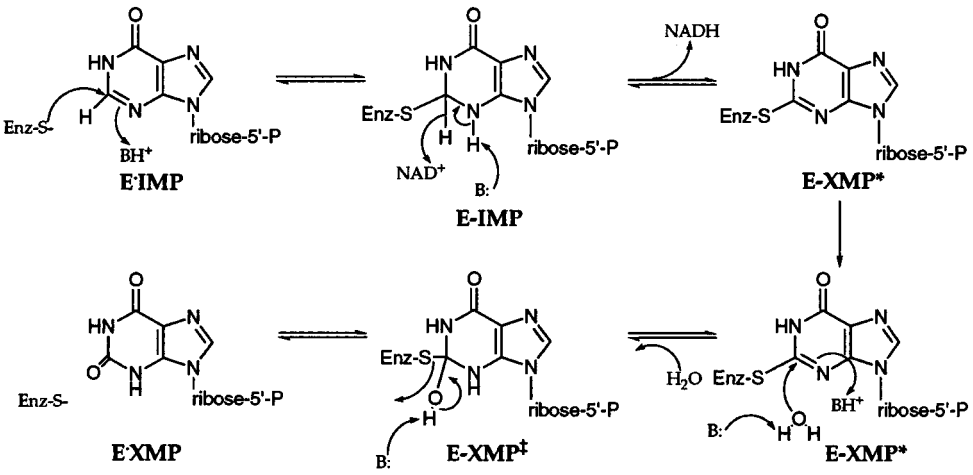


FIGURE 1: Mechanism of the IMPDH reaction.

Table 1: Conserved Carboxylate Residues in IMPDH[a]

| | | residue | | | | | | | | | | | |
|---|---|---|---|---|---|---|---|---|---|---|---|---|---|
| **classification** | **species**[b] | **13** (34) | **50** (71) | **54** (75) | **138** (162) | **200** (226) | **243** (269) | **248** (274) | **293** (319) | **338** (364) | **369** (395) | **373** (399) | **469** (500) |
| archae bacteria | *Methanococcus jannaschii* | D | D | E | D | D | D | D | D | D | E | G | E |
| | *Pyrococcus furiosus* | D | D | E | D | D | D | D | | D | E | K | E |
| eubacteria | *Myobacterium leprae* | D | D | E | D | D | D | D | D | D | E | E | E |
| | *Myobacterium tuberculosis* | D | D | E | D | D | D | D | D | D | E | E | E |
| | *Bacillus subtilis* | D | D | E | D | D | D | D | D | D | E | E | E |
| | *Escherichia coli* | D | D | E | D | D | D | D | S | D | E | E | E |
| | *Streptococcus pyogenes* | D | D | G | D | D | D | D | S | D | E | E | E |
| | *Haemophilus influenzae* | D | D | E | D | D | D | D | D | D | E | E | E |
| | *Acinetobacter calcoaceticus* | D | D | E | D | D | D | D | D | D | E | E | E |
| | *Borrelia burgdorferi* | D | D | E | T | N | D | D | D | D | E | E | E |
| eukaryotae | *Leishmania donovani* | D | D | E | D | D | D | D | D | D | E | E | E |
| | *Trypanosoma brucei brucei* | D | D | E | D | D | D | D | D | D | E | E | E |
| | *Saccharomyces cerevisiae* XII | D | D | E | D | D | D | D | D | D | E | E | E |
| | *Saccharomyces cerevisiae* VIII | D | D | E | D | D | D | D | D | D | E | E | E |
| | *Saccharomyces cerevisiae* XIII | D | D | E | D | D | D | D | D | D | E | E | E |
| | *Mus musculus* a | D | D | E | D | D | D | D | D | D | E | E | E |
| | *Mus musculus* b | D | D | E | D | D | D | D | D | D | E | E | E |
| | *Cricetulus griseus* | D | D | E | D | D | D | D | D | D | E | E | E |
| | *Homo sapiens* type 1 | D | D | E | D | D | D | D | D | D | E | E | E |
| | *Homo sapiens* type 2 | D | D | E | D | D | D | D | D | D | E | E | E |
| | *Mus musculus* type 1 | D | D | E | D | D | D | D | D | D | E | E | E |
| | *Drosophila melanogaster* | D | D | E | D | D | D | D | D | D | E | E | E |
| | *Pneumocystis carinii* | | D | E | D | D | D | D | D | D | E | Q | E |
| | *Arabidopsis thaliana* | D | D | E | Q | D | N | D | D | D | E | G | E |
| | *Tritrichomonas foetus* | E | Q | G | D | D | D | D | D | D | E | R | E |

[a] Sequences of 25 IMPDH proteins from various sources were compiled from a BLAST search of the National Center for Biological Information (NCBI) database using *E. coli* as the template. The sequences were aligned using PILEUP in the GCG software package, and carboxylate residues with ≥80% identity are shown. Numbering denotes the residue in the *E. coli* sequence, and the parentheses denote the corresponding residue number in the human type 2 sequence. [b] Species (NCBI identification number): *M. jannaschii* (1592337), *P. furiosus* (1170554), *M. leprae* (466944), *M. tuberculosis* (1449376), *B. subtilis* (124423), *S. pyogenes* (924848), *E. coli* (729847), *H. influenzae* (1170553), *A. calcoaceticus* (400057), *B. burgdorferi* (1352459), *L. donovani* (124425), *T. brucei brucei* (1078708), *S. cerevisiae* XII (665971), *S. cerevisiae* VIII (729848), *S. cerevisiae* XIII (577140), *M. musculus* a (425158), *M. musculus* b (124427), *C. griseus* (304517), *H. sapiens* type 1 (124417), *H. sapiens* type 2 (124419), *M. musculus* type 1 (392948), *D. melanogaster* (1170552), *P. carinii* (1272244), *A. thaliana* (1352458), *T. foetus* (1352865).

residues are the largest class of conserved residues among IMPDHs (Table 1), and several roles for carboxylate residues can be envisioned. Asp and Glu residues can act as general acids and/or bases, as shown in the mechanism in Figure 1. In addition, carboxylate residues are commonly involved in binding sites of nucleotides and nicotinamide cofactors (Montfort et al., 1990; Betts et al., 1994; Bellamacina, 1996). Carboxylate residues are also found in $K^+$ binding sites (Toney et al., 1993; Larsen et al., 1994; Liaw et al., 1995; Koster et al., 1996). Therefore, Asp and Glu residues emerge as good candidates for functionally important residues of IMPDH.

Here, an alanine scanning study investigates the roles of conserved Asp and Glu residues in *E. coli* IMPDH. We have identified five functionally important Asp/Glu residues. In addition, we have found that mizoribine 5′-monophosphate (MMP) is a transition state analog inhibitor of the IMPDH reaction (Figure 2). While this work was in progress, crystal structures for IMPDH from Chinese hamster and *T. foetus* were solved (Sintchak et al., 1996; Whitby et al., 1997). Since the coordinates of the *T. foetus* structure have only recently become available (and the hamster structure coordinates are not yet released), we will compare our results with the current structural information in the Discussion.

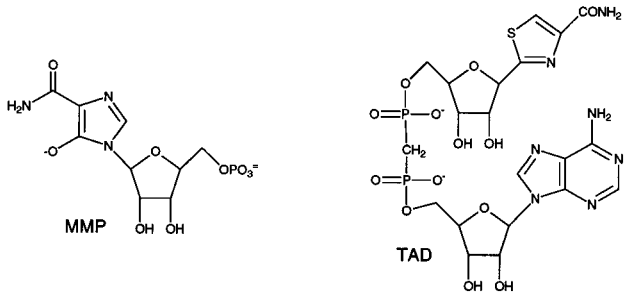


FIGURE 2: Mizoribine 5′-monophosphate (MMP) (left) and $\beta$-$CH_2$-tiazofurin adenine dinucleotide (TAD) (right).

## MATERIALS AND METHODS

*Materials.* IMP, $NAD^+$, XMP, and GMP were purchased from Sigma; glycerin was purchased from Fisher. The plasmid pJS49 containing the *E. coli gua*B gene was the gift of Dr. John M. Smith (Teideman & Smith, 1985). The p1 transducing lysate of p1-AB1157 and a recA-deficient donor strain STL134 were provided by Dr. Susan Lovett. MMP and EICARMP were the gift of Dr. Akira Matsuda, and TAD was the gift of Dr. Victor Marquez.

*Mutagenesis.* Asp54Ala, Asp138Ala, Asp243Ala, Glu373Ala, and Glu469Ala were constructed from pJS49 using the Quikchange kit (Stratagene, La Jolla, CA). The *E. coli gua*B gene was subcloned from pJS49 into pBluescriptKS$^+$ in order to construct Asp13Ala, Asp50Ala, Asp200Ala, Asp248Ala, Asp338Ala, and Glu369Ala using Kunkel mutagenesis (Kunkel, 1985). To ensure no undesired mutations had been introduced, the coding sequences of all IMPDH genes were sequenced using a PRISM Dyedeoxy Terminator Cycle Sequencing kit (Applied Biosystems, Inc.) and an Applied Biosystems 373A DNA sequencer at the Brandeis Sequencing Facility.

*LH3 Strain Construction.* A recombination-deficient strain of H712 was made using a p1 transducing lysate method (Miller, 1992). The donor strain (STL143, recAΔ306::Tn10) truncated the recA gene in the H712 genome with a tetracycline resistance gene. The new cell strain, LH3, showed an IMPDH-deficient, recombination-deficient phenotype (genotype, *F-fhuA2 lacY1 tsx-70 supE44? gal-6 λ-* trp-45 his-68 guaB22 tyrA2 rspL125 malT1(λR) xyl-7 mtl-2 thi-1 recAΔ306::Tn10).

*Expression of IMPDH.* Plasmids containing a wild-type or mutant IMPDH gene were transformed into LH3 cells using the TSS quick transformation method (Chung et al., 1989). Cells were grown for 48 h in 1.2 L LB broth with 100 $\mu$g/mL ampicillin and 20 $\mu$g/ml tetracycline at 37 °C with constant agitation.

*Purification of IMPDH.* Wild-type and mutant IMPDHs were purified by similar methods. The cells were harvested and washed three times with 50 mM Tris, pH 7.5, 1 mM DTT, and 10% glycerol (buffer A) and resuspended in 40 mL of buffer A and frozen at −80 °C. IMPDH was purified as previously described (Farazi et al., 1997) with the following modifications: a linear gradient of 0 to 2 M KCl was used to elute the protein from the Cibacron Blue Sepharose resin (Sigma) and a linear gradient of 0 to 1 M NaCl was used to elute the protein from the POROS CM Weak Cation Exchange column (PerSeptive Biosystems, Framingham, MA). Fractions containing IMPDH were pooled according to activity (wild-type) or SDS−PAGE (mutants). Enzyme was dialyzed against buffer A and stored at −80 °C. The enzyme preparations were judged >90% homogenous by SDS−PAGE stained with Coomassie Blue.

*Active Site Titration.* Protein concentrations for wild-type and all mutants except Asp338Ala were determined by active site titration with EICARMP (Wang et al., 1996). EICARMP does not inactivate Asp338Ala stoichiometrically; therefore, the concentration of Asp338Ala was determined using the Bio-Rad assay (IgG standard) calibrated from similar preparations of wild-type IMPDH.

*Native Gel Electrophoresis.* Wild-type and mutant proteins were subjected to native polyacrylamide gel electrophoresis to probe quaternary structure. A gel [7 in. (width) × 8 in. (length)] was prepared with 5% acrylamide (2.6% cross-linked) and 50 mM Tris, pH 8.0 and polymerized with 0.04% ammonium persulfate and 0.08% TEMED. Approximately 10 $\mu$g of each protein was loaded, and the gel was run at 95 V for 10 h at 4 °C in 50 mM Tris, pH 8.0, running buffer with three buffer changes. The gel was stained with Coomassie Blue to visualize the protein.

*Enzyme Assays.* Standard *E. coli* IMPDH activity assays contained 50 mM Tris, pH 8.0, 100 mM KCl, 3 mM EDTA, 1 mM DTT, 1 mM IMP, and 2.5 mM $NAD^+$. The reaction was initiated by the addition of enzyme, and the production of NADH ($\epsilon_{340} = 6.2$ $mM^{-1}$ $cm^{-1}$) was monitored at 25 °C using an Hitachi U-2000 spectrophotometer. To detect the activity of Asp338Ala, the production of NADH was monitored by fluorescence (excitation $\lambda$, 340 nm; emission $\lambda$, 460 nm) at 25 °C using either an Hitachi F-2000 fluorescence spectrophotometer or a PerSeptive Biosystems Cytofluor II multiwell plate reader. Concentrations of IMP and $NAD^+$ were varied appropriately for all wild-type and mutant $K_m$ determinations.

*EDC Inactivation.* Wild-type IMPDH was incubated in 50 mM Tris, pH 7.5, 10% glycerol, and 1 mM DTT at 25°C with 10 mM EDC, in the presence and absence of ethanolamine, and in the presence and absence of IMP. Controls contained no EDC. Aliquots were removed at appropriate times and assayed for enzymatic activity as described above. Rates of inactivation ($k_{inact}$) were determined from the slopes of semilogarithmic plots of the fraction activity vs incubation time.

*Data Analysis.* Michaelis−Menten parameters for wild-type and mutant IMPDHs were determined by fitting initial rate data to the Michaelis−Menten equation (1) and substrate inhibition equation (2):

$$v/E = k_{cat}A/(K_a + A) \quad (1)$$

$$v/E = k_{cat}B/(K_b + B + B^2/K_{ii}) \quad (2)$$

where $v/E$ is the initial velocity, $k_{cat}$ is the overall rate constant, $A$ is the IMP concentration, $K_a$ is the Michaelis−Menten constant for IMP, $B$ is the $NAD^+$ concentration, $K_b$ is the Michaelis−Menten constant for $NAD^+$, and $K_{ii}$ is the substrate inhibition constant for $NAD^+$.

Steady state parameters with respect to $NAD^+$ were derived by first determining apparent $k_{cat}$ values for the initial velocity vs IMP (eq 1) then replotting these values vs $NAD^+$ concentration (eq 2), resulting in the determination of $K_b$, $K_{ii}$, and $k_{cat}$. Similarly, the steady state parameters with respect to IMP were derived using the apparent $k_{cat}$ values for the initial velocity vs $NAD^+$ (eq 2), then replotting vs IMP concentration (eq 1) resulting in determination of $K_a$

and $k_{cat}$. The average of the $k_{cat}$ values was reported. The initial rate data from Asp13Ala, Asp50Ala, Asp248Ala, and Asp338Ala could not be fit to eq 2; the steady state parameters of these mutants were determined using eq 3 for sequential mechanism:

$$v/E = k_{cat}AB/(K_{ia}K_b + K_aB + K_bA + AB) \quad (3)$$

where $K_{ia}$ is the dissociation constant for IMP from the binary E·A complex.

Wild-type and all mutant enzyme activities were assayed at saturating IMP and $NAD^+$ concentrations and varied $K^+$ concentrations, and initial rate data were fit to eq 4:

$$v/E = k_{cat}[K^+]/(K_m + [K^+]) + C \quad (4)$$

where $K_m$ is the apparent Michaelis−Menten constant of $K^+$ and $C$ is a constant. All further characterization of Michaelis−Menten parameters and inhibition constants of Asp13Ala, Asp50Ala, and Glu469Ala was performed with 400 mM KCl in the assay buffer.

*Inhibitor Analysis*. For GMP and XMP, the values of $K_{is}$ were determined with constant $NAD^+$ concentrations and varied IMP and inhibitor concentrations. Initial rate data were fit to eq 5 for competitive inhibition:

$$v/E = k_{cat}A/[K_a(1 + I/K_{is}) + A] \quad (5)$$

where $I$ is the concentration of the inhibitor and $K_{is}$ is the dissociation constant of the E·I complex.

For TAD, the values of $K_{ii}$ were determined with constant IMP concentrations and varied $NAD^+$ and TAD concentrations. Initial rate data were fit to eq 6 for uncompetitive inhibition:

$$v/E = k_{cat}B/[K_b + B(1 + I/K_{ii})] \quad (6)$$

where $K_{ii}$ is the inhibition constant for TAD.

For MMP, the values of $K_i$ were determined using tight binding inhibitor and progress curve analysis. For tight binding inhibition, the values of $K_i$ were determined with constant $NAD^+$ concentrations and varied IMP and MMP concentrations. Initial rate data were fit to the Ackermann equation for competitive inhibition (eq 7) (Ackermann & Potter, 1949):

$$v = (k_{cat}/2)(E - K_iQ - 1) + [(K_iQ + I + E)^2 - 4IE]^{0.5} \quad (7)$$

where $v$ is the initial velocity, $E$ is the concentration of IMPDH active sites, and $Q$ is $[1 + (A/K_a)]$. Progress curve analysis was used when time-dependent inhibition was observed. The IMP and $NAD^+$ concentrations were constant while the MMP concentration was varied, and the reaction was monitored for 60 min. Data were analyzed by fitting to eqs 8, 9, and 10 (Orsi & Tipton, 1979; Hager et al., 1995):

$$v/E = (k_{off}k_{cat}/b)t + (Ik_{on}'k_{cat}/b^2)(1 - e^{-bt}) \quad (8)$$

$$k_{on} = k_{on}'Q \quad (9)$$

$$K_i = k_{off}/k_{on} \quad (10)$$

where $k_{off}$ is the dissociation rate constant of the E·I complex, $b = (Ik_{on}' + k_{off})$, $t$ is time, and $k_{on}'$ is the apparent association rate constant of the E·I complex. All data were fit to the appropriate equations using either KinetAsyst, Kaleidagraph, or Sigma Plot software.

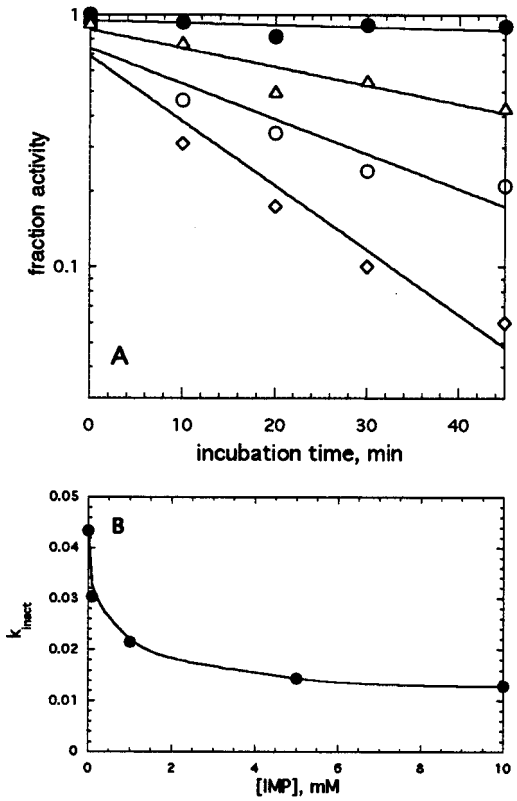


FIGURE 3: EDC inactivation and partial IMP protection of IMPDH. (A) *E. coli* IMPDH, 1.4 $\mu$M, was incubated with 10 mM EDC and various concentrations of ethanolamine, $[RNH_2] = 0$ (Δ), 50 (*o*), and 100 mM (◊), and enzyme activity was measured at appropriate intervals as described in Materials and Methods. Control (●) contained no EDC. (B) *E. coli* IMPDH, 1.4 $\mu$M, was incubated with 10 mM EDC, 100 mM ethanolamine, and varied concentrations of IMP. $k_{inact}$ was determined as described in Materials and Methods.

## RESULTS

*EDC Inactivation of IMPDH*. We tested the ability of carbodiimide reagents to inactivate IMPDH in order to provide evidence for the involvement of a carboxylate residue in the IMPDH reaction. Carbodiimide modification is commonly used to cross-link proteins and to identify exposed nucleophillic residues in proteins (Carraway & Koshland, 1972). Carbodiimide-modified carboxylate residues further react with amines to form amides; this reaction is diagnostic for the modification of carboxylates. IMPDH is inactivated by the carbodiimide EDC (Figure 3A). This inactivation is not caused by protein cross-linking as determined by SDS−PAGE of inactivated protein (data not shown). The rate of inactivation increases in the presence of ethanolamine (Figure 3A), which indicates that EDC inactivates IMPDH by modifying Asp and/or Glu residue(s). IMP partially protects IMPDH from EDC inactivation (Figure 3B). This observation indicates that EDC modifies a carboxylate residue outside the IMP binding site, perhaps in the $NAD^+$ or $K^+$ binding sites. In addition, since IMP protects IMPDH from inactivation by thiol reagents, this observation provides further evidence that EDC inactivation does not result from modification of the active site Cys (Brox & Hampton, 1968; Antonino et al., 1994; Huete-Perez et al., 1995). Thus, the

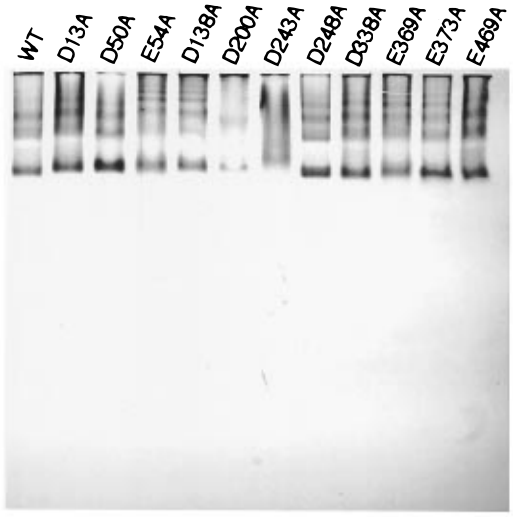


FIGURE 4: Native polyacrylamide gel of wild-type and mutant proteins. Each protein (10 $\mu$g) was analyzed on a 5% polyacrylamide gel at 4 °C as described in Materials and Methods.

inactivation of IMPDH by EDC suggests that a carboxylate residue is required in the IMPDH reaction.

*Conserved Carboxylates in E. Coli IMPDH*. Twelve Asp and Glu residues are conserved among IMPDHs from various sources (Table 1). Four of these residues, Asp248, Asp338, Glu369, and Glu469, are fully conserved. An additional three residues, Asp50, Asp200, and Asp243, are conserved in 24 of 25 sequences, and another three, Asp13, Asp54, and Asp138, are conserved in 23 of the sequences. It seemed prudent to include these 10 residues in the alanine scanning study. In addition, residue 373 was also included at the initiation of this study; the report of additional IMPDH sequences showed that this residue is conserved in only 20 of 25 sequences. Residue 293 is a Ser in *E. coli* and was therefore omitted from this study.

*Expression of IMPDH Mutants*. The *E. coli* strain H712 is commonly used to express recombinant IMPDH protein (Antonino & Wu, 1994; Farazi et al, 1997; Xiang et al., 1996; Sintchak et al., 1996). This strain lacks endogenous IMPDH activity, and H712 cells do not grow on minimal media in the absence of guanine (Nijkamp & De Haan, 1967). However, when these cells were transformed with a plasmid carrying an inactive *E. coli* IMPDH gene (Cys305 → Ala mutation), the transformants grew on minimal media. This observation suggests that recombination had occurred between the plasmid and chromosomal IMPDH genes regenerating a wild-type gene. Therefore, a recombination-deficient strain of H712, LH3, was constructed. LH3 cells transformed with a Cys305Ala IMPDH gene do not grow on minimal media. All mutant IMPDHs were expressed in LH3 cells. Interestingly, less active IMPDH mutants are expressed in greater quantities than wild-type IMPDH. All IMPDH mutants were purified using standard procedures as described in Materials and Methods.

*Quaternary Structure of the IMPDH Mutants*. The smallest active oligomer of *E. coli* IMPDH is a tetramer, although higher order enzyme aggregates are also formed (Powell, 1973; Gilbert et al., 1979). We analyzed the quaternary structure of the mutant IMPDHs by native PAGE (Figure 4). Both size and charge determine the migration of proteins in native PAGE (Hames & Rickwood, 1990), and this method can easily distinguish monomers from dimers and tetramers [see, for example, Maley et al. (1995)]. Wild-type IMPDH displayed multiple bands, as expected for an aggregating protein. The smallest molecular weight band migrated similar to catalase (Mm = 240 kDa), which is consistent with the molecular mass of a tetramer of *E. coli* IMPDH (Mm = 220 kDa) (data not shown). Like the wild-type enzyme, all of the mutant enzymes display multiple bands. The mobility of the smallest molecular mass band in the mutant enzymes is the same as wild-type in all cases, which indicates all of the mutant enzymes form tetramers. No faster migrating bands are observed for any of the mutant enzymes, further indicating that no monomeric or dimeric forms are observed in the mutants. The ability to form tetramers, and the failure to observe monomers or dimers, indicates that the mutations do not grossly perturb the structure of IMPDH. Interestingly, all of the mutant enzymes form higher order aggregate species similar to wild-type, although the aggregation pattern of Asp243Ala differs from the other proteins.

*Activity of Wild-Type E. coli IMPDH*. Table 2 summarizes the Michaelis−Menten parameters for wild-type IMPDH, as well as the values of $K_i$ for inhibition by IMP analogs XMP, GMP, and MMP and the $NAD^+$ analog TAD (Figure 2). Like IMPDH from other organisms, substrate inhibition is observed at high concentrations of $NAD^+$ for *E. coli* IMPDH (Hedstrom & Wang, 1990; Zhou et al, 1997; Xiang & Markham, 1996) (Figure 5). Presumably, this inhibition results from $NAD^+$ binding to the E-XMP* intermediate (Wu et al., 1995). No IMP substrate inhibition is observed. The values of $k_{cat}$, $K_m$, and $K_i$ for wild-type IMPDH are similar to those reported although previous characterizations of *E. coli* IMPDH did not account for $NAD^+$ substrate inhibition (Table 2) [$K_m$ (IMP) = 11 $\mu$M, $K_m$ ($NAD^+$) = 330 $\mu$M, $K_i$ (GMP) = 56 $\mu$M, (Gilbert et al., 1979); $K_m$ (IMP) = 13 $\mu$M, $K_m$ ($NAD^+$) = 190 $\mu$M, $K_i$ (GMP) = 82 $\mu$M, $K_i$ (XMP) = 130 $\mu$M (Powell et al., 1969)]. IMPDH is activated 100-fold in the presence of $K^+$, with an apparent $K_m$ for $K^+$ = 2.8 mM. Interestingly, MMP is a more potent inhibitor of *E. coli* IMPDH than mammalian IMPDHs [$K_i$ = 0.5 nM for *E. coli* (Table 2) versus $K_i$ = 4 nM for human IMPDH type II (Hager et al., 1995)], although TAD is a less potent inhibitor [$K_{ii}$ = 8.5 $\mu$M for *E. coli* versus $K_i$ = 0.2 $\mu$M for mouse IMPDH (Marquez et al, 1986)].

*Activity of the IMPDH Mutants*. Six mutants, Glu54Ala, Asp138Ala, Asp200Ala, Asp243Ala, Glu369Ala, and Glu373Ala, show no significant changes with respect to wild-type in all parameters assayed (Table 2). At least one parameter is changed by ≥10-fold in the remaining five mutants, Asp13Ala, Asp50Ala, Asp248Ala, Asp338Ala, and Glu469Ala. Surprisingly, the mutations have the greatest effect on the value of $K_i$ for MMP except in the case of Asp248Ala. The significance of this observation will be discussed below. The effects of the mutations on the other parameters are summarized as follows.

*Asp13Ala*. The Asp13 → Ala mutation causes a 38-fold increase in the value of $K_m$ for $K^+$. This mutation also decreases the value of $k_{cat}$ by 19-fold. No change is observed in the value of $K_m$ for IMP or in the values of $K_{is}$ for GMP and XMP. Unlike the other IMP analogs, the value of $K_{is}$ for MMP increases by 60-fold. While the $K_m$ for $NAD^+$ increases by 3-fold, the value of $K_{ii}$ for TAD is unchanged. No $NAD^+$ substrate inhibition is detected, which may signal a decrease in the accumulation of E-XMP* and is in keeping

Table 2: Kinetic Charaterization of *E. coli* IMPDH and Mutants (Unless Otherwise Noted, Error Was ≤15%)

| enzyme | $k_{cat}$ $s^{-1}$ | $k_{cat}/K_mK_m$ $[(sM2)^{-1} \times 10^7]$ | $K_m$ IMP ($\mu$M) | $K_m$ $NAD^+$ (mM) | $K_{ii}$ $NAD^+$ (mM) | $K_m$ $K^+$ (mM) | $K_{is}$ GMP ($\mu$M) | $K_{is}$ XMP ($\mu$M) | $K_i$ MMP (nM) | $K_{ii}$ TAD ($\mu$M) |
|---|---|---|---|---|---|---|---|---|---|---|
| wild-type | 13 | 11 | 61 | 2.0[a] | 2.8 | 2.8 | 86[a] | 130 | 0.5[c] | 8.5 |
| D13A[b] | 0.7 | 0.23 | 52[a] | 5.7 | na | 107 | 160 | 240 | 30[a,d] | 5.6 |
| D50A[b] | 1.2 | 0.48 | 61[a] | 4.1[a] | na | 48 | 670 | 930 | 60[a,d] | 1.7 |
| E54A | 14 | 6.7 | 87[a] | 2.4 | 3.6 | 6.0 | 230 | 230 | 1.8[a,c] | nd[f] |
| D138A | 7.1 | 12 | 44[a] | 1.4 | 4.5 | 4.3 | 78 | 72 | 1.1[a,c] | nd |
| D200A | 14 | 21 | 44 | 1.5 | 5.6 | 5.2 | 150 | 130 | 0.4[a,c] | nd |
| D243A | 12 | 11 | 56[a] | 2.0 | 7.5 | 4.0 | 88 | 120 | 0.7[c] | nd |
| D248A | 0.1[a] | 0.08 | 21[a] | 6.3[a] | na[e] | 35 | 64 | 30[a] | 40[a,d] | 210[a] |
| D338A | 0.02[a] | 0.0009 | 710[a] | 3.3[a] | na | 17 | 510 | 600[a] | 700[d] | nd |
| E369A | 7.1 | 6.7 | 53[a] | 2.0 | 5.5 | 7.2 | 300 | 340 | 1.9[a,c] | nd |
| E373A | 7.1 | 7.5 | 59 | 1.6[a] | 4.3 | 5.3 | 93 | 110 | 0.6[a,c] | nd |
| E469A[b] | 14 | 2.6 | 49 | 11 | 3.6 | 48 | 160 | 130[a] | 0.8[c] | 8.4[a] |

[a] Error was ≤25%. [b] Kinetic constants determined at 400 mM KCl. [c]Progress curve analysis. [d]Tight binding analysis. [e]na, not applicable. [e]nd, not done.

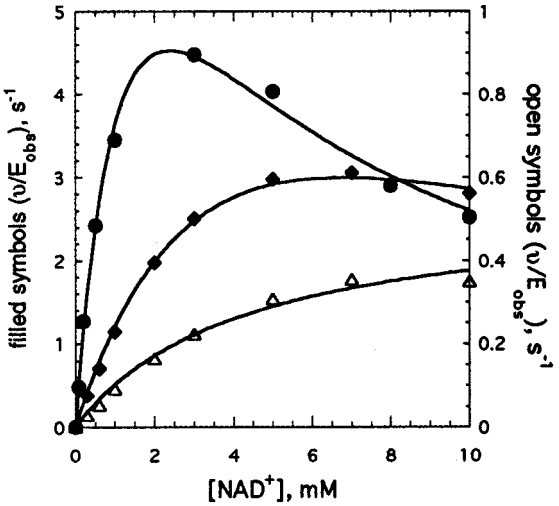


FIGURE 5: $NAD^+$ substrate inhibition. Enzyme activity was assayed with 50 mM Tris, pH 8.0, 400 mM KCl, 3 mM EDTA, 1 mM DTT, and 1 mM IMP (wild-type contained 100 mM KCl). The values of the initial rates of NADH formation by wild-type (●) and Glu469Ala (◆) (left axis) were fit to eq 2, which describes substrate inhibition. The values of the initial rates of NADH formation by Asp13Ala (△) (right axis) were fit to eq 1 for Michaelis−Menten kinetics.

with the decrease in the value of $k_{cat}$ (Figure 5). Since large changes are observed in $K^+$ affinity and $k_{cat}$, we suggest that Asp13 is involved in $K^+$ activation and may be a ligand at the $K^+$ binding site.

*Asp50Ala*. The Asp50 → Ala mutation also causes an 17-fold increase in the value of $K_m$ for $K^+$ and 10-fold decrease in the value of $k_{cat}$. Interestingly, Asp50Ala exhibits sigmoidal kinetics at a low concentration of $K^+$, although Michaelis−Menten kinetics are observed at high $K^+$ concentrations (data not shown). This mutation has wide ranging and apparently contradictory effects. For example, while no change in the value of $K_m$ for IMP is observed, the values of $K_{is}$ for GMP and XMP increase by 7-fold. Once again, a larger effect is observed in the value of $K_{is}$ for MMP, which increases by 120-fold. While a 2-fold increase is observed in the value of $K_m$ for $NAD^+$, the value of $K_{ii}$ for TAD decreases 5-fold. No $NAD^+$ substrate inhibition is detected, in keeping with the decrease in $k_{cat}$. Like Asp13, we tentatively assign Asp50 to a monovalent cation binding site since the largest effect (not including MMP affinity) is on $K^+$ activation.

*Asp248Ala*. The Asp248 → Ala mutation causes a 130-fold decrease in the value of $k_{cat}$. In addition, the value of $K_{ii}$ for TAD increases by 25-fold, and the value of $K_m$ for $NAD^+$ increases by 3-fold. This mutation also increases the value of $K_m$ for $K^+$ by 13-fold. No $NAD^+$ substrate inhibition is detected, again in keeping with the decrease in $k_{cat}$. While a 3-fold decrease is observed in the value of the $K_m$ for IMP and a 4-fold decrease in the $K_{is}$ for XMP, no change in the $K_{is}$ for GMP is observed. Once again, a greater perturbation is observed in the value of the $K_i$ for MMP, which increases by 80-fold. We assign this residue to the $NAD^+$ site, since this mutation causes a large decrease in the value of $k_{cat}$ and a substantial increase in the value of $K_i$ for TAD, while smaller changes are observed in the values of $K_i$ for IMP analogs.

*Asp338Ala*. While another laboratory was unable to detect activity in the analogous mutant of Chinese hamster IMPDH (Sintchak et al., 1996), we can detect activity in Asp338Ala mutant of *E. coli* IMPDH. This activity is not the result of wild-type contamination: a greater than $10^3$-fold increase in the value of $K_i$ for MMP is observed and EICARMP does not rapidly inactivate Asp338Ala as seen with wild-type enzyme. The Asp338 → Ala mutation has a large effect on the value of $k_{cat}$, which decreases by 600-fold. The Asp338 → Ala mutation increases the value of $K_m$ for IMP by 12-fold and the values of $K_{is}$ for GMP and XMP by approximately 6-fold. No change in the value of $K_m$ for $NAD^+$ is observed. A 6-fold increase in the value of $K_m$ for $K^+$ is also noted. The large change in the value of $k_{cat}$ and the smaller changes in the values of $K_m$ for IMP and $K_{is}$ for XMP and GMP indicate that Asp338 may be an acid-base catalyst in the IMP binding site.

*Glu469Ala*. The Glu469 → Ala mutation increases the value of $K_m$ for $K^+$ by 17-fold. The only other change observed is in the value of $K_m$ for $NAD^+$, which increases by 5-fold. This mutation does not affect the values of $k_{cat}$ and $K_m$ for IMP, the value of $K_{ii}$ for $NAD^+$ substrate inhibition, or the value of $K_{ii}$ for TAD. These observations suggest that Glu469 is near a $K^+$ binding site. However, the failure to observe a change in $k_{cat}$ suggests that Glu469 is probably not a ligand for $K^+$.

*MMP Inhibition.* As mentioned above, much larger increases were observed in the values of $K_i$ for MMP than in the values of $K_m$ for IMP or $K_{is}$ for GMP and XMP. The increases in the values of $K_i$ for MMP appeared to correlate with decreases in values of $k_{cat}$. This observation suggests

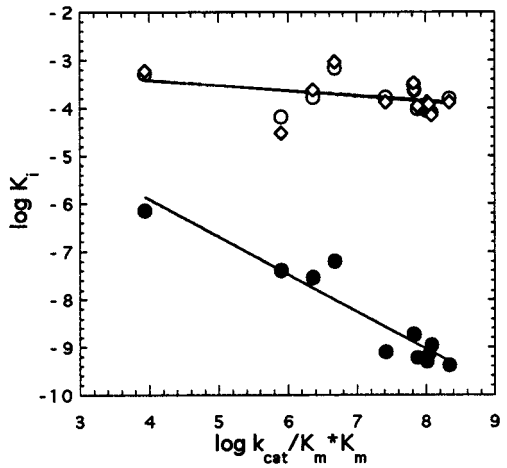


FIGURE 6: Correlation of $K_i$ and $k_{cat}/K_m*K_m$ values. $K_{is}$ GMP (○), $K_{is}$ XMP (◇), $K_i$ MMP (●). Lines are from linear regression analysis.

that MMP may be a transition state analog of the IMPDH reaction. Such a transition state analogy can be confirmed by demonstrating that the values of $K_i$ correlate with the values of $k_{cat}/K_m$ for a series of analogous substrates and inhibitors (Wolfenden, 1969; Bartlett & Marlowe, 1983). Alternatively, a correlation between the values of $K_i$ and $k_{cat}/K_m$ for a single substrate/inhibitor pair and a series of mutant enzymes can be used (Phillips et al., 1992). For a bisubstrate enzyme such as IMPDH, the affinity of a transition state analog will correlate with $k_{cat}/K_mK_m$ (Wolfenden, 1969). In order to test the transition state analog hypothesis, the $K_i$ of MMP was plotted versus $k_{cat}/K_mK_m$ for each of the mutant enzymes (Figure 6). A good correlation is observed ($r^2 = 0.9$) with a slope of 0.8. No such correlation is observed for the values of $K_{is}$ for GMP and XMP ($r^2 = 0.2$ and 0.1, respectively) (Figure 6) or the $K_{ii}$ for TAD or when the $K_i$ for MMP is plotted against $K_m$ for IMP (data not shown).

## DISCUSSION

*Comparison with the Crystal Structures of IMPDH*. We have assigned functions to five IMPDH residues: Asp13, Asp50, and Glu469 are involved in $K^+$ binding; Asp13 and Asp50 are possible ligands at a $K^+$ binding site, Asp248 is involved in $NAD^+$ binding and Asp 338 is a likely general acid-base catalyst at the IMP binding site. In addition, we found that the mutation of Glu54, Asp138, Asp200, Asp243, Glu369, and Glu373 have only minor effects on IMPDH function. The recent reports of crystal structures of IMPDH allow us to map some of these residues onto the protein structure.

Three crystal structures of IMPDH have been solved: the E-XMP*·MPA complex of IMPDH from Chinese hamster (Sintchak et al., 1996) and the apoenzyme and E·XMP complex of *Tritrichomonas foetus* IMPDH (Whitby et al., 1997). The coordinates of *T. foetus* IMPDH were generously provided prepublication, while the coordinates of Chinese hamster IMPDH are not yet available. Both groups report that IMPDH has an $\alpha/\beta$ barrel structure. Common to $\alpha/\beta$ barrel proteins, the active site of IMPDH is composed of loops C-terminal to the $\beta$ strands of the barrel (Farber & Petsko, 1990). The loop after $\beta$8 forms a flap which covers the active site. Similar flaps control access to the active sites in other $\alpha/\beta$ barrel proteins (Joseph et al., 1990). In addition, IMPDH contains an unique 150 residue insertion between $\alpha$2 and $\beta$3. This "subdomain" is missing in IMPDH from *Borrelia burgdorferi* (Zhou et al., 1997). Sintchak et al. (1996) report that the subdomain can be deleted without loss of IMPDH activity, although no details of this experiment have been presented. Thus, the subdomain is not required for IMPDH activity. The active site is adjacent to the subunit interface and near the N- and C-termini of the neighboring subunit in the tetramer. Unfortunately, both structures contain large regions of disorder, including portions of the flap, the subdomain and the N- and C-termini. Much of the active site of *T. foetus* IMPDH is also disordered, including the active site Cys.

The six residues which are not required for IMPDH activity should be located far from the active site. Indeed, two of these residues, Asp138 and Asp200, are found in the subdomain, and another, Asp243, is found on the N-terminal end of the $\beta$ barrel and, thus, far from the active site. Although Glu369 and Glu373 are in the C-terminal loops of the $\beta$ sheets, they are nevertheless at least 16 Å from XMP in the structure of *T. foetus* IMPDH. Therefore, five of the residues which are not required for IMPDH activity are all located far from the active site. However, Glu54 is also found in the C-terminal loops; the analogous residue, Gly64, is 12 Å from XMP in *T. foetus* IMPDH, which suggests that the side chain of Glu54 could be quite close to the active site. The failure to observe a significant effect for this mutation is somewhat surprising.

*Asp248 Is in the $NAD^+$ Site*. The Asp248 → Ala mutation causes a 25-fold increase in the value of $K_{ii}$ for TAD and a 120-fold decrease in the value of $k_{cat}$, which suggests that Asp248 is in the $NAD^+$ site. Asp248 is found in the MPA binding site of IMPDH (Sintchak et al., 1996), and MPA is known to bind in the nicotinamide portion of the $NAD^+$ binding site (Hedstrom & Wang, 1990). Therefore, both mutagenesis and structural data suggest that Asp248 is in the $NAD^+$ binding site.

*Asp338 May be a General Acid-Base Catalyst*. The Asp338 → Ala causes the greatest decrease in $k_{cat}$ (600-fold). This change is accompanied by comparatively modest increases in the values of $K_m$ for IMP and $K_{is}$ for GMP and XMP (≤12-fold). These observations suggest that Asp338 contributes more to catalytic activity than substrate binding. Thus, it is tempting to propose that Asp338 acts as a general acid-base in the IMPDH reaction. However, Asp338 makes hydrogen bonds to the 2′ and 3′ hydroxyls of both E-XMP* and E·XMP (Sintchak et al., 1996; Whitby et al., 1997). Presumably, Asp338 makes these same interactions with IMP, which would seem to prevent this residue from acting as a general acid-base. However, Asp338 appears to be linked to N3 of E-XMP* by a network of bound water molecules. It is intriguing to speculate that Asp338 acts as a general acid or base via this water network. Alternatively, Asp338 may have a different orientation in the E·IMP complex. Indeed, the conformation of enzyme bound IMP is different than E-XMP*: enzyme-bound IMP has a $C_{2'}$-endo ribose conformation whereas E-XMP* has a $C_{3'}$-endo conformation (Xiang & Markham, 1996). Experiments are in progress to further delineate the role of Asp338 in the IMPDH mechanism.

*Monovalent Cation Activation of IMPDH*. Mutations of the remaining three residues, Asp13, Asp50, and Glu469, appear to exert their effects primarily through $K^+$ binding.

The mutation of both Asp13 and Asp50 decrease the value of $k_{cat}$ as well as the affinity for $K^+$. Therefore, we believe that both Asp13 and Asp50 could be ligands at the $K^+$ binding site. In contrast, the mutation of Glu469 does not decrease $k_{cat}$, although this mutation increases the value of $K_m$ for $K^+$ by 17-fold. Therefore, it is likely that Glu469 interacts with the ligands of the $K^+$ site. Most monovalent cation binding sites contain an Asp or Glu residue (Toney et al., 1993; Larsen et al., 1994; Liaw et al., 1995; Koster et al., 1996). However, alkali metal binding sites are extremely difficult to identify crystallographically. Unfortunately, the IMPDH structures provide limited insight into monovalent cation activation. No monovalent cation sites were located in the *T. foetus* structure, in keeping with the its low dependence on monovalent cations. Intriguingly, Asp50 is substituted with Gln in *T. foetus* IMPDH. While Sintchak et al. (1996) claim to identify a monovalent cation binding site in Chinese hamster IMPDH, only one ligand, the carbonyl of the active site Cys, was specified. The remaining ligands include four main chain carbonyls, three of which are somewhere in the C-terminal region, and a water molecule. Thus, neither Asp13 nor Asp50 appear to be ligands at this site, although it is possible that Glu469 is nearby. Unfortunately, Glu469 is disordered in the crystal structure of *T. foetus* IMPDH. However, both Asp13 and Asp50 are discernible (Whitby et al., 1997). Asp13 is located in the subunit interface while Asp50 is near the active site; these two residues are separated by at least 30 Å across the monomer or the nearest subunit. Therefore, it is likely that Asp13 and Asp50 demarcate two distinct $K^+$ binding sites.

*Transition State Analogy of MMP*. MMP is the active metabolite of the immunosuppressive agent mizoribine and a potent inhibitor of IMPDH. In the course of these experiments we noticed that the mutations have a much greater effect on the value of the $K_i$ for MMP than on the $K_i$ of the other IMP analogs. Moreover, the changes in the values of $K_i$ for MMP correlate with the changes in the values of $k_{cat}/K_mK_m$ (Figure 6). This observation identifies MMP as a transition state analog for the IMPDH reaction. No such correlation is observed for the values of $K_{is}$ for GMP and XMP or $K_{ii}$ for TAD, indicating that these compounds are ground state analogs, as expected. The slope of the correlation is 0.8; this slope may indicate that MMP recapitulates 80% of transition state character. It seems likely that the negative charge of MMP mimics the charge which develops on N3 of IMP during the IMPDH reaction (Figures 1 and 2).

*Conclusions.* We identified five functionally important Asp/Glu residues in *E. coli* IMPDH: Asp248 is involved in $NAD^+$ binding, Asp338 may be an acid-base catalyst, Asp13 and Asp50 may be ligands at two distinct $K^+$ binding sites, and Glu469 is near a $K^+$ binding site. In addition, we demonstrate that MMP is a transition state analog for the IMPDH reaction.

## ACKNOWLEDGMENT

We would like to thank Geoff Stamper for initiation of the EDC work, Joyce Keck for her work on the $K^+$ dependence of wild-type and the Asp50Ala mutant, and Frank Whitby and C. C. Wang for generously providing the coordinates of the *T. foetus* structure. Special thanks go to Rebecca Myers for the DNA sequencing of all mutants and Dr. Susan Lovett and Vincent Sutera for their assistance with the recombination-deficient cell strain construction.

## REFERENCES

Ackermann, W. W., & Potter, V. R. (1949) *Proc. Soc. Exp. Biol. Med. 72*, 1−9.
Allison. (1993) *Immunol. Rev. 136*, 5−28.
Anderson, J., & Sartorelli, A. (1968) *J. Biol. Chem. 243*, 4762−4768.
Antonino, L. C., & Wu, J. C. (1994) *Biochemistry 33*, 1753−1759.
Antonino, L. C., Straub, K., & Wu, J. C. (1994) *Biochemistry 33*, 1760−1765.
Atkins, C., Shelp, B., & Storer, P. (1985) *Arch. Biochem. Biophys. 236*, 807−814.
Bartlett, P. A., & Marlowe, C. K. (1983) *Biochemistry 22*, 4618−4624.
Bellamacina, C. (1996) *FASEB J. 10*, 1257−1269.
Betts, L., Xiang, S., Short, S. A., Wolfenden, R., & Carter, J. C. W. (1994) *J. Mol. Biol. 235*, 635−656.
Brox, L., & Hampton, A. (1968) *Biochemistry 7*, 2589−2596.
Carraway, K. L., & Koshland, D. E., Jr. (1972) *Methods Enzymol. 25*, 616−623.
Chung, C. T., Niemela, S. L., & Miller, R. H. (1989) *Proc. Natl. Acad. Sci. U.S.A. 86*, 2172−2175.
Farazi, T., Leichman, J., Harris, T., Cahoon, M., & Hedstrom, L. (1997) *J. Biol. Chem. 272*, 961−965.
Farber, G. K., & Petsko, G. A. (1990) *Trends Biochem. Sci. 15*, 228−234.
Gilbert, H., Lowe, C., & Drabble, W. (1979) *Biochem. J. 183*, 481−494.
Hager, P. W., Collart, F. R., Huberman, E., & Mitchell, B. S. (1995) *Biochem. Pharm. 49*, 1323−1329.
Hames, B. D., & Rickwood, D. (1990) *Gel Electrophoresis of Proteins*, Oxford Univeristy Press, NY.
Hedstrom, L., & Wang, C. C. (1990) *Biochemistry 29*, 849−554.
Heyde, E., Nagabhushanam, A., Vonarx, M., & Morrison, J. (1976) *Biochim. Biophys. Acta 429*, 645−660.
Huete-Perez, J. A., Wu, J. C., Whitby, F. G., & Wang, C. C. (1995) *Biochemistry 34*, 13889−13894.
Hupe, D., Azzolina, B., & Behrens, N. (1986) *J. Biol. Chem. 261*, 8363−8369.
Joseph, D., Petsko, G. A., & Karplus, M. (1990) *Science 249*, 1425−1428.
Koster, J. C., Blanco, G., Mills, P. B., & W., M. R. (1996) *J. Biol. Chem. 271*, 2413−2421.
Kunkel, T. A. (1985) *Proc. Natl. Acad. Sci. U.S.A. 82*, 488−492.
Larsen, T. M., Laughlin, L. T., Holden, H. M., Rayment, I., & Reed, G. H. (1994) *Biochemistry 33*, 6301−6309.
Liaw, S. H., Kuo, I., & Eisenberg, D. (1995) *Protein Sci. 4*, 2358−2365.
Link, J. O., & Straub, K. (1996) *J. Am. Chem. Soc. 118*, 2091−2092.
Maley, F., Pedersen-Lane, J., & Changchien, L. (1995) *Biochemistry 34*, 1469−74.
Marquez, V. E., Tseng, C. K. H., Gebyehu, G., Cooney, D. A., Ahluwalia, G. S., Kelley, J. A., Dalal, M., Fuller, R. W., Wilson, Y. A., & Johns, D. G. (1986) *J. Med. Chem. 29*, 1726−1731.
Miller, J. H. (1992) *A Short Course in Bacterial Genetics*, Cold Spring Harbor Laboratory Press, NY.
Montfort, W. R., Perry, K. M., Fauman, E. B., Finer-Moore, J. S., Maley, G. F., Hardy, L., Maley, F., & Stroud, R. M. (1990) *Biochemistry 29*, 6964−6977.
Nijkamp, H. J. J., & De Haan, P. G. (1967) *Biochem. Biophys. Acta* 31−40.
Orsi, B. P., & Tipton, K. F. (1979) *Methods Enzymol. 63*, 159−183.
Phillips, M. A., Kaplan, A. P., Rutter, W. J., & Bartlett, P. A. (1992) *Biochemistry 31*, 959−963.
Powell, G., Rajagopalan, K. V., & Handler, P. (1969) *J. Biol. Chem. 244*, 4793−4797.
Powell, G. F. (1973) *Biochemistry 12*, 1592−1595.
Robins, R. (1982) *Nucleosides Nucleotides 1*, 35−44.
Segel, I. H. (1975) *Enzyme Kinetics*, Wiley-Interscience, NY.

Sintchak, M. D., Fleming, M. A., Futer, O., Raybuck, S. A., Chambers, S. P., Caron, P. R., Murcko, M. A., & Wilson, K. P. (1996) *Cell 85*, 921−930.

Streeter, D. G., Witkowski, J. T., Khare, G. P., Sidwell, R. W., Bauer, R. J., Robins, R. K., & Simon, L. N. (1973) *Proc. Nat. Acad. Sci. U.S.A. 70*, 1174−1178.

Teideman, A. A., & Smith, J. M. (1985) *Nucleic Acids Res. 13*, 1303−1306.

Toney, M. D., Hohenester, E., Cowan, S. W., & Jansonius, J. N. (1993) *Science 261*, 756−758.

Verham, R., Meek, T. D., Hedstrom, L., & Wang, C. C. (1987) *Mol. Biochem. Parasit. 24*, 1−12.

Wang, W., Papov, V. V., Minakawa, N., Matsuda, A., Biemann, K., & Hedstrom, L. (1996) *Biochemistry 35*, 95−101.

Weber, G. (1983) *Cancer Res. 43*, 3466−3492.

Whitby, F. G., Luecke, H., Kuhn, P., Somoza, J. R., Huete-Prez, J. A., Phillips, J. D., Hill, C. P., Fletterick, R. J., & Wang, C. C. (1997) *Biochemistry 36*, 10666−10674.

Wolfenden, R. (1969) *Nature 223*, 704−705.

Wu, J. C., Carr, S. F., Antonino, L. C., Papp, E., & Pease, J. H. B. (1995) *FASEB Abstr. 9*, 472.

Xiang, B., & Markham, G. D. (1996) *J. Biol. Chem. 271*, 27531−27535.

Xiang, B., Taylor, J. C., & Markham, G. D. (1996) *J. Biol. Chem. 271*, 1435−1440.

Zhou, X., Cahoon, M., Rosa, P., & Hedstrom, L. (1997) *J. Biol. Chem. 272*, 21977−21981.

BI9714161